



WPI

Progressive Molding of Soft Robots for Ocean Conservation

A Major Qualifying Project Report
Submitted to the Faculty of
WORCESTER POLYTECHNIC INSTITUTE
In partial fulfillment of the requirements for the
Degree of Bachelor of Science

by:

Dilce Oliveira, Robotics Engineering
Owen Rouse, Electrical and Computer Engineering
Sara Frunzi, Mechanical Engineering

Spring 2024

Advisor:

Markus Nemitz, Assistant Professor of Robotics Engineering

This report represents work of three WPI undergraduate students submitted to the faculty as evidence of a degree requirement. WPI routinely publishes these reports on its web site without editorial or peer review. For more information about the projects program at WPI, see <http://www.wpi.edu/Academics/Projects>.

Abstract

Coral reefs, which house a quarter of the ocean's biodiversity, are under threat due to plastic waste. Underwater remotely operated vehicles (ROVs) equipped with a gripper can be used to collect macroplastics caught in the reefs. Due to the frail nature of coral, these expeditions require sensitive manipulation; grippers made from soft rubbers and plastics allow for manipulation with minimal risk to the surrounding environment. However, fabrication of these grippers is often complex, time-consuming, and necessitates manual labor. We present a novel fabrication technique - progressive molding - to streamline the process of creating soft gripper components. By using this method, we can create complex shapes that cannot be made in a single cycle of replica molding. Additionally, the process uses materials that are too soft to be FDM 3D printed with standard machines. We designed a soft gripper with actuators that could be fabricated via progressive molding. Finally, we attached the gripper to a four degree-of-freedom robotic arm on a commercially available ROV to remotely clean coral reef systems.

Acknowledgements

We would like to thank all of the members of the Robotic Materials Group who assisted us in our project and learning goals. In particular, we would like to thank Cem Aygül for his advice and feedback throughout the MQP. We would also like to thank Professor Markus Nemitz for his guidance on this project.

Contents

1	Introduction	5
2	Background	6
2.1	Biodiversity, Coral Reefs, and Threats Thereof	6
2.2	Current Coral Restoration Methods	7
2.3	Soft Robots	8
2.3.1	Design Factors in Soft Robotics	8
2.3.2	Manufacturing of Soft Robots	9
2.4	Underwater Manipulators	10
2.5	Current Waterproof Servos and Methods	11
3	Progressive Molding a Soft Gripper	12
3.1	Concept	12
3.2	Experimental Process	12
3.2.1	FDM Printing with PVA Filament	12
3.2.2	Printing on Silicone	14
3.2.3	Progressively Molding an Actuator	15
3.3	Designing Soft Gripper	17
4	Design of BlueROV2 System Equipped with 4 DoF Arm	18
4.1	Concept	18
4.2	Fabricating Servo Casings	19
4.2.1	Future Improvements	23
4.3	Fabricating Robot Arm	23
4.3.1	Future Improvements	26
5	Integration	26
5.1	Attaching the Arm to the ROV	26
5.2	Programming The Arm	28
5.2.1	Future Programming Iterations	29
6	Conclusion	30

List of Figures

1.1	Progressive molding process used to design soft gripper for manipulator on BlueROV2.	6
2.1	Coral restoration methods.	8
2.2	Caged grippers by (a) [1] and (b) [2]. Parallel grippers by (c) [3] and (d) [4]. Claw grippers by (e) [5], (f) [6], (g) [7], (h) [8], and (i) [9].	11
3.1	Results of testing printing parameters of PVA.	14
3.2	Results of testing parameters of printing on top of silicone.	15
3.3	Pneunet CAD render (left) and sectional view render of pneunet and mold with labeled parameters (right).	16
3.4	Pneunet patterning being progressively molded (top), side and top views (middle), and fully encased and cured (bottom).	16
3.5	Bellow design with parameter variables labeled (left), bellow being progressively molded (middle), partial bellow fabricated via progressive molding (right).	17
3.6	CAD rendering of the soft gripper.	17
4.1	Proposed robotic solution concept	18
4.2	Schematic of Dynamixel X430-W350-R servo	19
4.3	Case Lid, Dynamixel Servo, Servo Horn Extension, Case. Listed top to bottom.	22
4.4	Assembled final case iteration, fabricated using SLA 3D printing technology.	23
4.5	Link has been skeletonized to reduce weight, increase geometric strength, and reduce drag.	24
4.6	Link with slots for cable ties, press fit bearing (Bottom Middle), and servo horn extension fitment (Bottom Right).	25
4.7	Final Arm Iteration, fabricated using FDM 3D printing technology.	26
5.1	Base of the arm that connects to ROV. Four M5 screw holes, stability bearing on the outside, and servo horn attachment in the center.	27
5.2	Robotic Arm attached to BlueROV2 with soft gripper.	28
5.3	Electronic footprint of the system. Gamepad controller, Tether, Raspberry Pi, U2D2, Robotic Arm. Left to Right.	28

List of Tables

- 3.1 Static Print Parameters. 13
- 3.2 Pneunet Design Specifications (all units mm). 15
- 3.3 Bellow Design Specifications. 17

- 4.1 Design Iterations and Considered Factors 21

Chapter 1

Introduction

Robotic manipulators, arms, and end-effector systems are used to pick up and manipulate objects [10]. The equivalent for humans are hands and arms, which can dexterously pick up, move, and rotate objects. Underwater robots use robotic manipulators to collect marine life specimens or unwanted objects in the ocean [11, 8, 9]. Underwater remotely operated vehicles (ROVs) have become increasingly popular for underwater observations and specimen collection, as they allow for humans to remotely interact with the environment and observe specimens in situ [9]; however, they often lack qualities needed to harmlessly interact with wildlife in the ocean.

Current manipulator end effectors include parallel pincer-type grippers, cage grippers, biomimetic hands, and claw-type grippers. Despite the variety in shapes and types, but are too rigid to interact carefully with wildlife or to pass through tight spaces without causing damage to their surroundings [10, 9, 12]. Soft grippers, which can be made from low shore-hardness plastics and rubbers, have found purpose as a cost-effective solution due to their high adaptability, safety, and ability to conform to small spaces and different environments [12, 9]. The sensitive interactions between grippers and the environment are apt for manipulating marine specimens with minimal risk to the specimen and surroundings [6, 9].

In the case of cleaning macro plastics from coral reefs, the coral's outer shell can be easily damaged by the material used to create traditional rigid grippers. A soft gripper would be able to conduct direct contact with the coral without causing such abrasions to its surface [9, 11]. As such, soft grippers that can be attached to ROVs open countless avenues for marine life research and underwater cleanup initiatives [6, 7]. However, fabrication of these grippers is often complex, costly, time-consuming, and/or necessitates manual labor [13, 14, 15]. We present a new technique for fabricating soft components, used in this case for fabricating soft actuators of an underwater gripper. This technique, known as progressive molding, combines the advantages of FDM printing and replica molding.

The process of progressive molding begins much like that of replica molding. The key difference is that instead of printing the entire mold, assembling it, and filling it with silicone after the process, we pause the print at key points and insert silicone mid-print. Traditional replica molding has the advantage of using very low shore hardness materials, but has limited geometry, as it cannot create hollow or thin features without secondary processing. Conversely, FDM 3D printing can create detailed and complex geometry but is much more

limited in its available materials.

To accomplish the goal of creating a system to remotely clean coral reef systems, we attach a 4-degree-of-freedom robotic arm, derived from the Open Manipulator X (RMX 52) equipped with a soft gripper to a commercially-available ROV from Blue Robotics, the BlueROV2, as demonstrated in Figure 1.1. The soft gripper is designed to have a progressively molded and 3d printed end effector. The use of progressive molding will allow for a complex shape and actuation method, while allowing for the gripper to remain entirely soft.

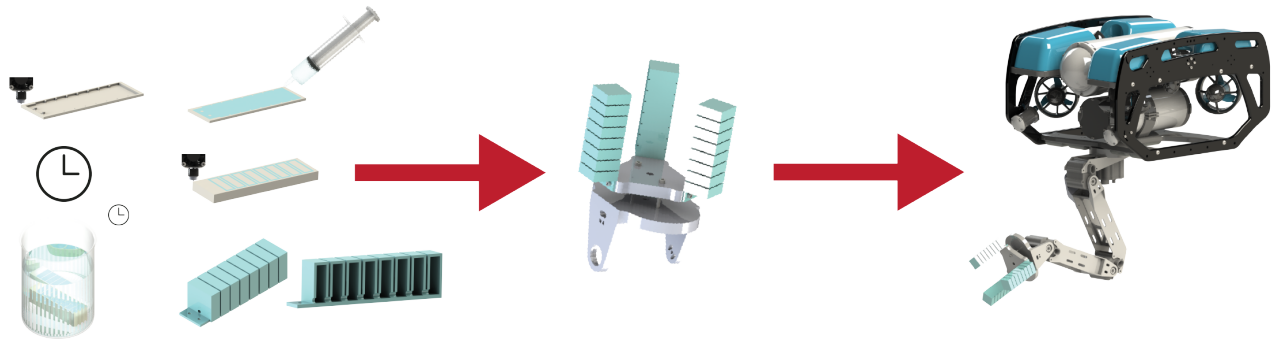


Figure 1.1: Progressive molding process used to design soft gripper for manipulator on BlueROV2.

Chapter 2

Background

2.1 Biodiversity, Coral Reefs, and Threats Thereof

Coral reefs, while only taking up 1% of the ocean floor, house 25% of all of the ocean’s biodiversity [16]. They are responsible for protecting shorelines, can be harvested for medicine, and help trap CO_2 in the ocean to combat the rising temperature of the environment [16]. In the last 30 years, half of the oceans’ corals have been lost to climate change through coral bleaching caused by the rising climate temperature, or forced erosion caused by plastic waste; since 1990, The Great Barrier Reefs have lost over half of its corals, some of which were over 50 million years old [17].

Each year, an estimated 11 billion plastic items are entangled in the Asia-Pacific region’s

coral reefs, home to over half of the world’s coral reefs [16]. The likelihood of disease in their ecosystem increases from 4% to 89% when corals are in contact with plastics causing a rapid decline in their reproductive cycles, in addition to the abrasive properties of debris paired with ocean currents [18].

2.2 Current Coral Restoration Methods

The efforts that currently exist to tackle the effect of plastic waste on coral reefs revolve largely around human-led volunteer clean-ups, where divers remove plastic debris from coral reefs by hand. Organizations, such as Dive Friends Bonaire and Padi Aware, partner with local organizations, schools, and local brands to host beach-specific clean-ups on the coasts of nearby communities. Dive Friends Bonaire hosts 4 clean-ups per year and partners with Padi Aware to record their findings in the ‘Dive Against Debris’ database hosted by Padi Aware. This database allows certified volunteer divers to record any marine debris they have removed from the ocean in both solo and group dives. Divers are encouraged to catalog their findings and participate in smaller clean-up sequences as individuals. The database assists in keeping track of other efforts to clean debris and can help marine biologists learn more about how plastic waste is impacting marine life.

According to the database, Dive Friend Bonaire was able to cover 43,055 square feet over 5 hours during their most recent clean up [19]. The divers were split into smaller teams of two or more to cover a wider area. Each team was briefed on their mission of carefully collecting plastic waste while being mindful of marine life, avoiding physical contact with the coral reefs, and leaving any pieces of debris that are inhabited by marine life.

The organizations also participate in educational efforts to teach the broader community about how plastic waste ends up on coral reefs, and how sustainability practices can assist in keeping coral reefs free of plastic debris. These efforts, while marginally effective, require an intense amount of community planning, donations of time, equipment, and resources, and rely heavily on volunteers to become certified divers with the skills necessary to participate in the clean up. A robotic system would allow for remote maintenance of coral reefs to keep them clean in an efficient and cost-effective manner without the need for multiple volunteers with extensive scuba diving training.



Figure 2.1: Coral restoration methods.

2.3 Soft Robots

2.3.1 Design Factors in Soft Robotics

Zhang, et. al. [20] identify material, structure, actuation, function, and intelligence as five critical design factors in soft robotics; for our purposes of developing a soft gripper, material, structure, and actuation are most important. Flexible materials in soft robotics are defined by their “Shore Hardness” shown in Figure 1. Silicones fall on the softer end of the spectrum, with common shore hardnesses ranging from approximately 00-10 to 40A, and are typically used for casting or molding [21, 22, 23]. Commercially available thermoplastic polyurethanes (TPUs) used for 3D printing are available as soft as 60A in standard filaments and 45A in pellets [24, 25, 26]; these materials are harder in comparison to silicones but are much softer than typical engineering materials such as hard plastics and metals.

Actuation– the factor that enables basic motion– is generally motor-less in soft robots, so other methods of actuation have become popular via necessity [27]. Actuation methods include/soft fluidic actuators (SFAs), smart material actuators, and cable-driven systems [28, 15]. SFAs are made from soft materials and use fluids, such as air or water, to change the pressure inside the actuator, causing the soft material to twist or bend. Examples of SFAs include bellows, internal combustion actuators, and pneumatic networks (PneuNets) [15]. Smart material actuators use stimuli-responsive materials or shape memory materials to change the shape of a component under certain circumstances, such as an environmental change in temperature or magnetism. Cable-driven components are usually soft or multi-jointed and embedded with cables, which, when pulled by an outside force, cause bending or rotation of the component. Cable actuators are often used in manipulators and continuum robots [29, 30].

Finally, we consider the structure of soft robots; structure may inform material and actuator choice, or vice versa. Structural design can include stiffness and compliance of mechanisms and components in a robot, assembly after fabrication, and mechanical design. Stiffness and compliance can, again, be attributed to material choice by using soft or smart materials; however, designing compliant mechanisms from rigid materials is also a possibility

through altering components' shapes and thicknesses [20]. Compliant and tunable stiffness mechanisms have the benefits of desired movement in a manner that fully rigid systems may be unable to do simply, and rigid strength or "locking" at times that entirely soft systems cannot attain [31, 32]. Another structural tactic in soft and conformable robots includes origami and kirigami. Origami refers to the Japanese art of folding paper into shapes and kirigami refers to a similar art style, which involves cutting paper to make shapes; soft roboticists have adapted these art forms to design structures that can flex while maintaining some structural stiffness [33, 34, 35]. These are only a few of the structural tactics and considerations utilized in soft robotics; beyond design factors lie manufacturing considerations.

2.3.2 Manufacturing of Soft Robots

Some of the most common methods include fused-deposition modeling (FDM) 3D printing, stereolithography (SLA) 3D printing, direct inkjet printing, and replica molding [20, 28, 15]. Each has its benefits and disadvantages, including but not limited to cost, material variety, and ability to create complex geometry.

Replica Molding

The process of replica molding, or casting, involves creating a rigid mold, often via FDM printing. Once the mold is created and fabricated, elastomer parts can be mixed and poured into the mold, then left to set before demolding [14]. Once complete, the part is a replica of its negative mold, hence the name "replica molding." These parts can be created in a singular mold, or several parts then attached in a post-manufacturing process [28, 15]. Such is the case for creating soft fluidic actuators, as replica molds cannot create a fully enclosed space using a single molding. While multi-part molds may be desirable to generate complex features, the interface between two casted parts is a common spot for mechanical failure due to the relatively low adhesion strength between the parts [13]. However, this process does have the advantage of adding additional materials in casted parts, such as strain-limiting layers in soft actuators [15, 36].

This method of manufacturing has the benefits of utilizing extremely low shore hardness elastomers, but the caveats are that it can be a lengthy process and cannot produce complex geometry such as hollow spaces without additional assembly steps [13] [14]. The resolution and tolerance of casted parts are directly related to the resolution of the mold, so it does not have advantages or disadvantages in this domain when compared to the other common methods we discuss.

Fused Deposition Modeling (FDM) 3D Printing

FDM Printing has become popular in the past two decades for rapid prototyping and manufacturing; soft robotics is no outlier to this trend. FDM involves wire or thermoplastic filament, such as earlier-mentioned TPUs, being pushed through a heated nozzle, melted, and extruded to form layers of a three-dimensional object [13, 27] [14]. FDM printing also has the advantage of being able to incorporate multiple materials of differing hardnesses

in a single print with commercially available 3D printers, though the variety and softness of these materials are somewhat limited, with the softest common filament measuring 60A shore hardness [27] [filaflex]. Another caveat of the FDM process, for fluidic-based and underwater robots, is airtightness; FDM printing can attain airtight structures, but the process requires precisely tuned printing and design parameters [37]. FDM 3D printing is quicker than replica molding and allows for complex geometries that replica molding cannot attain in a single process, but the softness of available FDM materials is much more limited— a sometimes-damning factor in soft robotics [14, 38]. Compared to stereolithography printing and direct ink writing, FDM 3D printing has a lower resolution, with the smallest common nozzles used being 0.1mm [13].

Stereolithography (SLA) 3D Printing

Stereolithography (SLA), otherwise known as vat polymerization, is a method of 3D printing that involves dipping a print bed into photocuring resin and using a projected light to cure the resin in the shape of a layer of a three-dimensional shape [13]. This photopolymerization is done repeatedly for layers with resolution as small as under 100 micrometers [39]. This technique has the advantage of higher resolution and the ability to create complex geometry, but material selection is limited, with commercially-available resins ranging from 80A to 50A shore hardness [40] and the disadvantage of being more costly than FDM printing [15].

Direct Inkjet Printing (DIP)

Another common approach in soft robotics is Direct Inkjet Printing (DIP). DIP uses photocurable inks and jet droplets of diameter 10-150 micrometers onto a build surface. A UV light is used to photocure that layer of material before depositing the next layer [28, 41, 42, 20]. Like FDM printers, DIP polyjets can have multiple nozzles and deposit multiple materials, making them suitable for soft wearables and electronics-based soft systems [41]. With a wide range of materials and excellent resolution, many would think that DIP is the primary fabrication method in soft robotics, but it has the drawbacks of expensive machine maintenance, nozzle limitations, and being less user-friendly than other methods we discuss [42, 13, 43].

2.4 Underwater Manipulators

As we previously discussed, soft grippers are becoming increasingly popular for underwater manipulation due to their ability to hold delicate specimens without harming them [9]. This section explores the variety of underwater grippers in the literature. Adapting from [12], we classify common underwater grippers into three types: cage, claw, and parallel grippers. Cage grippers can be characterized by the complete enclosure of their specimens, such as grippers by [1] and [2]. Parallel grippers are much like crab or insect pincers, with two fingers that move towards each other to grasp an object; these can be seen in [3] and [4]. Claw grippers are the most common type of gripper and have three or more fingers used to grasp items. These may be connected with a mesh or thin material, or the fingers may be completely separate. Fingers may also come together to a point or intermesh with each

other. Examples of claw grippers include [5], [6], [7], [8], and [9]. All three of these gripper types are shown in Figure 2.2.

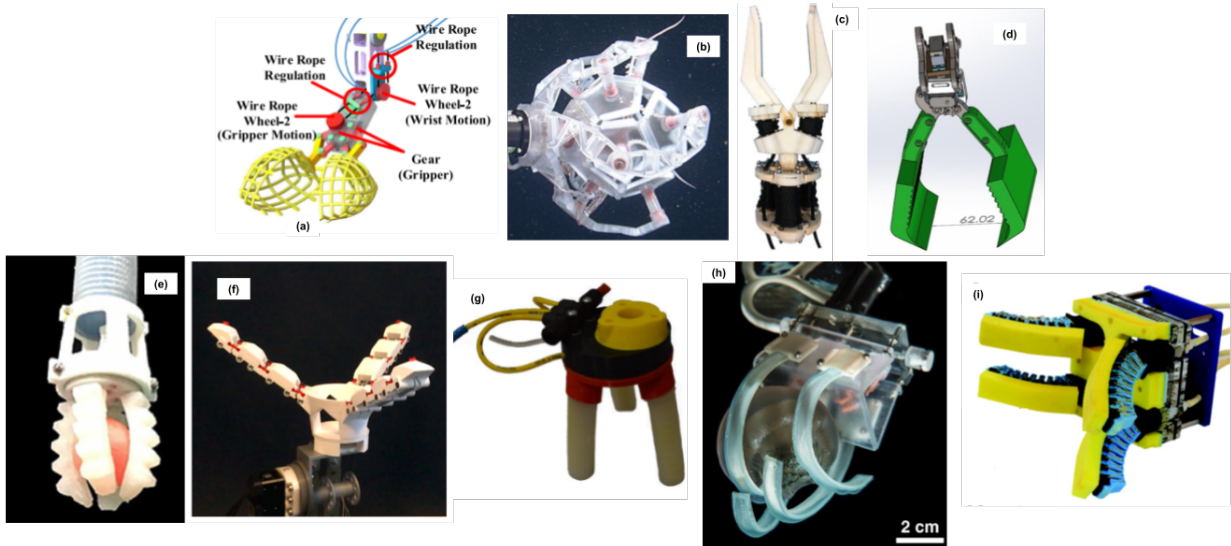


Figure 2.2: Caged grippers by (a) [1] and (b) [2]. Parallel grippers by (c) [3] and (d) [4]. Claw grippers by (e) [5], (f) [6], (g) [7], (h) [8], and (i) [9].

2.5 Current Waterproof Servos and Methods

Coral reefs are typically found anywhere between 20 - 40 meters below the water’s surface [17]. As such, a waterproof servo option must withstand these depths for elongated periods, with the inclusion of a factor of safety. On the current market, most “waterproof” servos are intended for minor depths and brief periods, far less than the requirements of this project. These can be seen in hobby-grade servos intended to be used in RC vehicles[44]. Waterproof servos that fulfilled the requirements were often expensive and not tailored to our specific use case, the lowest and most appropriate being the SER-20xx by Blue Trail Engineering at \$395 per servo[45].

Waterproofing methods commonly used, such as oil filling and epoxy coating, were not intended to be used at the depth required for this project. These techniques and many others are typically meant for use on inexpensive servos, as the mentality is shifted towards replace-ability, rather than reliability. These practices are typically used on hobby-grade servos, which have a very common shape that is generally sealed to dust, allowing for simple applications of waterproofing. This project had the unique challenge of focusing on both reliability and repeatability with the need for a more complex and robust servo.

Chapter 3

Progressive Molding a Soft Gripper

3.1 Concept

We created the concept of progressive molding as a solution to the need for a cost-effective, streamlined fabrication process to develop complex structures from soft materials. The process involves progressively FDM printing partial molds of a structure, filling it with silicone, and printing the next segment on top. This process is repeated until a full mold is printed and filled with silicone. Progressive molding integrates the positive aspects of FDM printing and replica molding while eliminating their major limiting factors. This method allows for soft actuators to be easily fabricated from very soft materials (trials tested with 10A silicone) with no post-processing assembly.

3.2 Experimental Process

3.2.1 FDM Printing with PVA Filament

Polyvinyl Alcohol (PVA) is a commercially available, low-cost FDM 3D printing material for dissolvable supports in dual-extrusion printers. Previous studies have examined printing parameters for PVA on MakerBot printers, PVA adherence to Acrylonitrile Butadiene Styrene (ABS) [46], and dissolution rate of PVA [47]. However, print parameters vary from machine to machine, especially given the advances that have been made in FDM printing technology since the release of MakerBot printers. Furthermore, PVA and ABS adhesions and dissolution rates may be good starting points for adhering to PLA or dissolving the PVA from silicone, but we must systemize the printing of PVA on our printers first.

In this work, we carefully tuned the printing parameters of PVA on a Prusa MK4 with a 0.4mm nozzle by printing a 20x20x20mm calibration cube, pausing for two minutes at

30% and 60% of the part’s completion to simulate the cooling endured during the time it may take to inject silicone in a progressive molding experiment. The calibration cube is sliced in PrusaSlicer, changing layer height, nozzle temperature, and extrusion multiplier in consecutive experiments. Unchanging parameters are shown in Table 3.1. After the part has been printed, it is removed from the print bed and examined for indicators of breakage between layers where silicone could slip through in the progressive molding process, particularly at the layers where a pause occurred. We conducted this experimental process with PVA that has been exposed to moisture and sunlight then placed in a dehumidifier as well as brand new PVA placed inside a dehumidifier.

Table 3.1: Static Print Parameters.

Fill Density (%)	5
Maximum Print Speed (mm/s)	30
Bed Temperature (C)	60
Idle Hot End Temperature (C)	130

Layer Height

The first parameter we tested was the height of print layers. Smaller layer heights often correspond with better adhesion between layers and finer detail finish in printed parts. We printed calibration cubes with layer heights of 0.4mm, 0.2mm, and 0.1mm, theorizing that the smaller layer heights would reduce delamination after pause layers due to increased time when the hot end is near the cooled layer. The nozzle temperature during this stage was 190C and the extrusion multiplier was 1.

Nozzle Temperature

After determining the optimal layer height, we tested the hot end temperatures. The recommended temperature range from the PVA manufacturer was 190-210C. We tested our calibration cubes at nozzle temperatures of 180, 190, and 200C based on past experiences with printing PVA on the Prusa MK4, but expected that higher temperatures would promote adhesion between layers. The layer height during these tests was 0.1mm and the extrusion multiplier was 1.

Extrusion Multiplier

The extrusion multiplier is, as it sounds, a multiplier to the extrusion rate of filament out of the nozzle, with 1 being the default, ≥ 1 extruding more filament, and ≤ 1 extruding less filament. We hypothesized that a larger extrusion multiplier would enhance adhesion due to more filament and more surface area provided for adhesion, and tested extrusion multipliers of 1, 1.05, and 1.15. The layer height during these tests was 0.1mm and the hot end temperature was 180C.

Results

After concluding testing, we found that a layer height of 0.1mm, a hot end temperature of 180C, and an extrusion multiplier of 1.15 provided the best results. Many other combinations resulted in delamination and breaking, particularly at the pause and bed layers as shown in Figure 3 below.

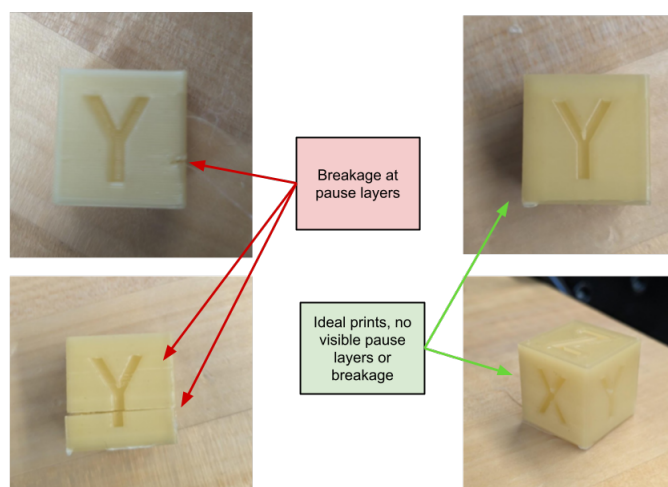


Figure 3.1: Results of testing printing parameters of PVA.

3.2.2 Printing on Silicone

The second, and largest, challenge to navigate was FDM printing on top of silicone, as there is no record of this being done in the literature. For this set of experiments, a cylinder shell was 3D printed from PVA using the parameters previously established. After the shell was printed, it was filled with silicone. After a predetermined amount of time, the print was resumed to print a circular disk on top of the silicone with no attachment to the previous layers of PVA. To standardize these trials, the cylinder shell was designed to hold exactly 5 mL of silicone. Additionally, the silicone was always pre-mixed and pre-measured using a plastic syringe.

Like the previous experiments, there were several parameters being changed, one at a time: fan speed, print speed, cure status, and silicone fill level. We tried having the fan speed at 100%, 50%, and 0%. Similarly, we tested the print speed at 30 mm/s (the original speed we were printing at) and 15 mm/s for the first three layers of printing on top of the silicone. For cure status, we examined printing on fully uncured (printed immediately after filling), partially cured (printed after 20% of cure time passed), and fully cured (printed after full cure time passed) silicone. Finally, we measured the silicone fill level, such that filling the cylinder shell with 4.9mL of silicone meant that the fill level was 0.2mm (2 print layers) less than the last layer printed, and filling with 5mL of silicone meant that the fill level was flush with the last layer printed. When printing on top of fully cured silicone, we attempted

to improve adhesion by using methods seen for bed adhesion in FDM printing, including utilizing glue, hairspray, and an “ABS Slurry.”

We found that a 0% fan speed and 15 mm/s print speed for the first 3 layers after silicone fill yielded the best results. Additionally, printing on top of fully cured silicone and using a silicone adhesive on the first layer produced a disk that adhered well to the silicone surface.

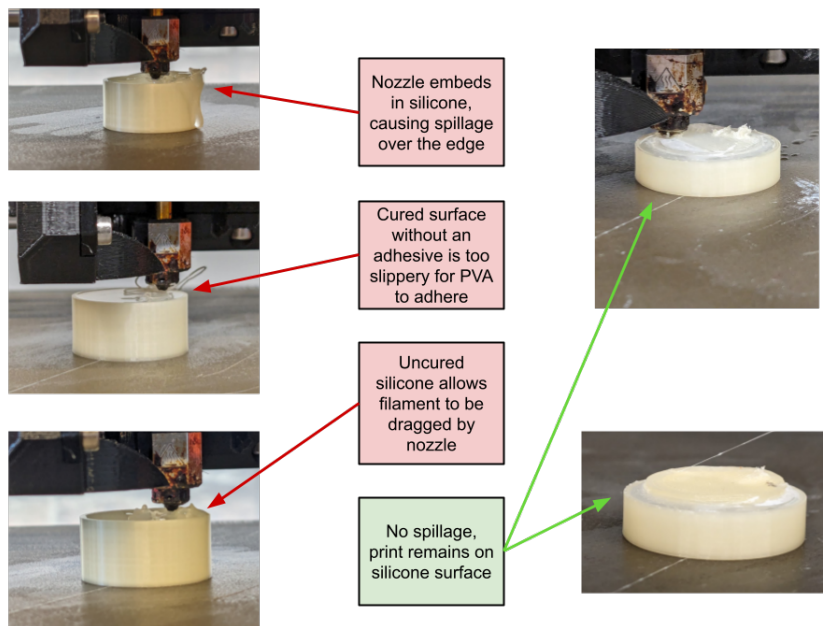


Figure 3.2: Results of testing parameters of printing on top of silicone.

3.2.3 Progressively Molding an Actuator

After the initial proof of concept, we attempted to create a soft actuator using progressive molding. The pneunet would have 8 chambers, with the specifications shown in Table 3.2:

Table 3.2: Pneunet Design Specifications (all units mm).

Chamber width	w	6
Chamber height	h	21.6
Wall thickness	t	1.5
Gap between chambers	g	1
Air channel diameter	d	2

We had successful trials of singular cycles of progressive molding, shown by PVA patterning encased in silicone in Figure 3.4. However, the printer we were using, the Prusa MK4, had documented problems un-pausing after extended periods [48]. The progressive molding process requires allowing the silicone to cure completely before continuing printing, which resulted in the Prusa MK4 being unable to continue the process for more than one cycle.

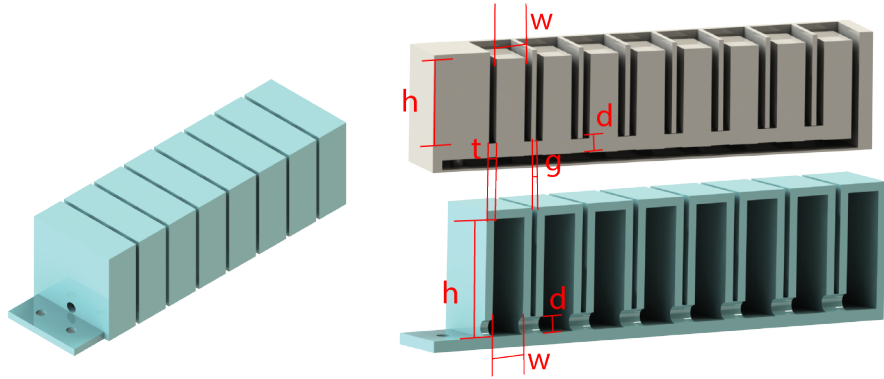


Figure 3.3: Pneunet CAD render (left) and sectional view render of pneunet and mold with labeled parameters (right).

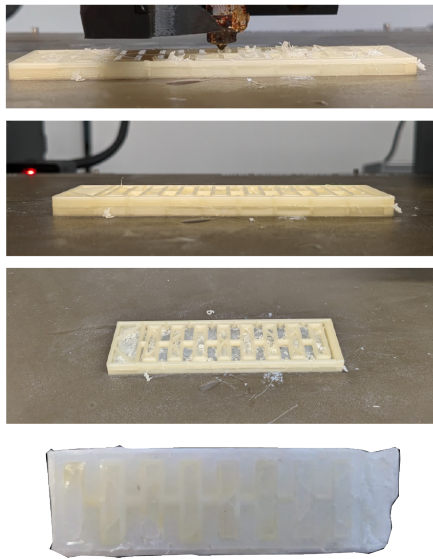


Figure 3.4: Pneunet patterning being progressively molded (top), side and top views (middle), and fully encased and cured (bottom).

Due to time constraints, we opted to create a bellows actuator instead of a pneunet, as the smaller design would still be practical while needing less time for the silicone to cure. Unfortunately, we were unable to produce a complete bellows actuator at the time of writing this paper due to time constraints. However, a partial actuator with the following specifications was progressively molded, as shown in Figure 3.5:

Table 3.3: Bellow Design Specifications.

Chamber width	w	12.5 mm
Wall thickness	t	2 mm
Angle of chambers	a	15 deg
Air channel diameter	d	1 mm

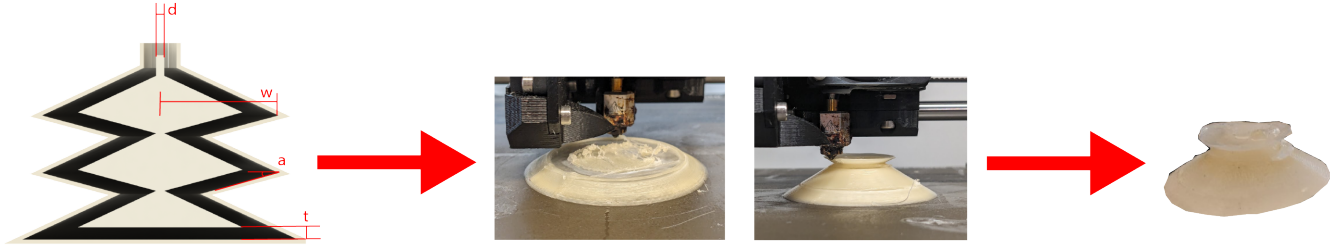


Figure 3.5: Bellow design with parameter variables labeled (left), bellow being progressively molded (middle), partial bellow fabricated via progressive molding (right).

3.3 Designing Soft Gripper

As previously stated, the motivation of this project lies in creating a soft gripper for an underwater remotely operated vehicle. This gripper was designed to be a claw type, with three hydraulically actuated pneunets as appendages (Figure 3.6). These pneunets were the same design that was used in the progressive molding trials and was attached to a two-stage rigid wrist printed from PLA. The first stage connects to a servo horn for pitch rotation, containing a hole in the center to constrain the actuation tubing. The second stage constrained the pneunets in a triangular pattern. Additionally, the pneunets were actuated via a peristaltic pump using ambient water to actuate, eliminating dangerous pressure differential or the need for air compressors and pumps.

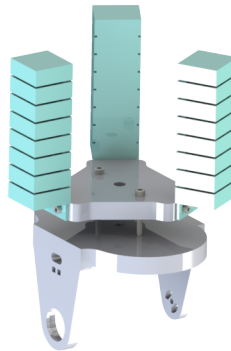


Figure 3.6: CAD rendering of the soft gripper.

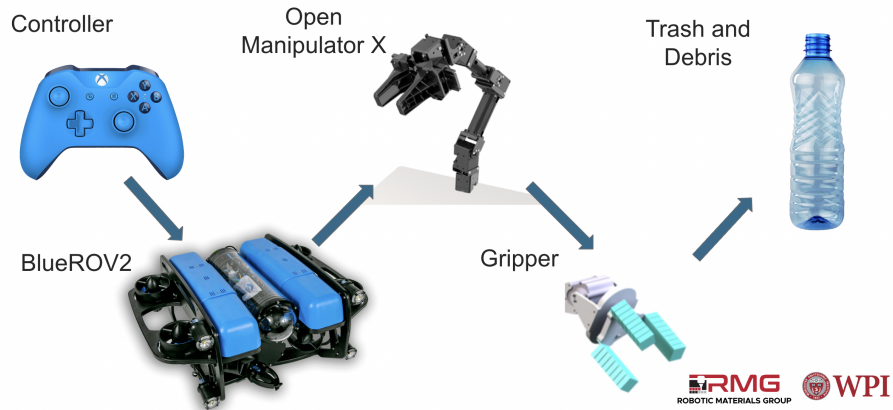


Figure 4.1: Proposed robotic solution concept

Chapter 4

Design of BlueROV2 System Equipped with 4 DoF Arm

4.1 Concept

Through this project, we sought to make an easily controllable, cost-efficient, diver-free system to accomplish the task of cleaning corals in a manner safe for marine life. A former project in our lab utilized an original Blue Robotics Blue ROV 2, an underwater remotely operated vehicle. The ROV came packaged together, but not built, and was equipped in its standard configuration with six Blue Robotics T200 thrusters, a high-definition low-light camera mounted onto a servo to allow for frame manipulation, four dimmable Lumen Lights, and a depth rating of up to 300 meters. Using the pieces sorted from the former project, we reconstructed and modified the Blue ROV 2 to include 2 additional thrusters for 6-degree-of-freedom control and feedback stability. A robotic arm was then fabricated and added to the undercarriage of the ROV frame. The robot's position is controlled using a gamepad controller, and the robotic arm is controlled using an additional controller.

The complex geometry of the X430 servos added an extra challenge for standard waterproofing methods such as epoxy coating and oil filling, which made sealing the servo motors themselves a risky and potentially costly task. Instead, we shifted our objective towards creating an external barrier from the servos from the outside water.

Each casing is comprised of three distinct parts: the lid, servo horn extension, and casing body. The body was designed to conform to the unique shape of the Dynamixel X430-W350-R servos and was fitted with chamfers that help the servo slide into the casing and remain in place. The ridges inside of each casing were sanded down to achieve the correct tolerances for each servo. Fillets were used to allow for easy installation of the servos and to mitigate the tearing of o-rings during the installation process. The body also has through holes to allow for screws to be inserted for added protection. The lid has a channel for wires to be inserted through and was designed to hold a 608 bearing to assist in the integration with the robotic arm links. Inspired by the waterproofing methods used by Blue Robotics in their Blue ROV2, the servo casings were also designed to use custom-fit O-rings to provide a water-tight seal. Both the servo horn and lid had two layers of O-rings which were covered in grease to form a water-tight seal. In the final production of the casings, they were filled with mineral oil to ensure that the inside can remain hydrophobic as an added measure of protection. A ‘venting screw’ allows for the casings to be closed with the mineral oil still inside letting out the excess incompressible fluid and closed with the screw to be fully sealed.

Given the short timeline, our objective was to design various iterations of the casings quickly for continuous testing to monitor progress. The primary criterion was to ensure the casings were watertight. This metric was heavily reliant on the fabrication method and material choices. Due to time and budget constraints, the casings needed to be fabricated in a cost- and time-efficient manner that allowed the testing and production process to be easily repeatable.

A second consideration was the weight of the casings. As this arm is to be mounted to the bottom of an ROV, we had to be concerned with weight to avoid additional strain on the robot’s thrusters, reducing battery life and maneuverability. Weight also plays a role in recovery from instability. If the arm adds too much weight, buoyancy will be affected, potentially rendering the robot negatively buoyant in the case of a mechanical failure.

The rigidity of the enclosure also needed to be taken into consideration. For the enclosure to seal, the flex of the material needs to be minimal to give the O-rings the best chance to seal. The rigidity of the material directly impacts the performance of the arm, increasing “slop” in the joints as the part becomes less rigid.

In our iterations of testing, we considered fabrication via Fused Deposition Modeling (FDM 3D) printing, Stereolithography (SLA) 3D printing, and CNC milling of various materials such as nylon, aluminum, and stainless steel billets. The casings went through a total of nine different FDM & SLA 3D printed iterations as outlined in the table below.

Table 4.1: Design Iterations and Considered Factors

Iteration	Changes Made	Remaining Challenges
1	Thick walls, BlueRobotics Penetrator Bolts, Mounting holes for easy attachment	Excessive/inconsistent screw placement, poor servo horn implementation, lack of sealing surfaces
2	Added sealing O-ring groove, Geometry modifications for heat dissipation	Redundant sealing methods, complexity of O-ring channel
3	Simplified O-ring channel, Enhanced support for servo horn, Improved screw placement	Bulkiness, excessive material usage
4	Roasted housing for easier insertion, Switched to insertion-based sealing, Reduced wall thickness and screw count	Sealing method for servo horn, Optimal distance between walls and servo
5	Reduced casing size, Standardized mounting options, Added chamfers for smoother insertion	Tolerance errors for servo horn and screws
6	Adjusted tolerances, Added chamfers for safety	Slim servo horn
7 (Final)	Refined tolerances for SLA printing, Improved O-ring fitment	-

Each casing attempt went through a thorough analysis process to assess if it would be a viable testing option. The first cases to be water tested were iterations #6 and #7. These iterations were printed using a Prusa MK3 FDM printer and PLA filament. To test the merit of the housing design, the PLA test prints were covered in marine-grade epoxy, attached to a QYSEA FiFish drone, and transported to the bottom of the pool (14 ft depth) below the surface for 30 minutes. For the majority of the testing period, the cases appeared to be sealed and no visible air bubbles could be seen from the surface. At the 28-minute mark air bubbles began to surround the cases and they were pulled back to the surface to assess

their performance. Neither case had succeeded as both of their materials were too porous. These tests solidified that FDM printing would not be a viable option for the final housing fabrication.

We intended for final fabrication methods to be switched to CNC milling aluminum, as the material would be waterproof, but due to restraints in the cost associated with material sourcing, fabrication outsourcing, and lead time, we chose to fabricate via SLA printing. The first SLA prototype was successful in remaining watertight after its first water test; however, the tolerances needed to be adjusted to account for the printer's alignment to fit the servos correctly.

The final casings were SLA printed using a Formlabs Form 3L printer. After the first round of casings were printed, they were ultimately unable to fit the servos due to slight tolerancing issues. The casings needed a very tight fit to remain waterproof, and thus even the slightest variation would make it difficult to fit the casings properly. When the casings were printed for the next iteration, there were unforeseen issues with the printers. The next several rounds of prints were not able to be printed securely. Some casings had holes on the side panels, the flat surfaces had curves and various inexplicable bumps or misshaping, and the inside collapsed onto itself during the printing process. It was unclear what was causing these issues as the first run of the prints seemed to print without issue. The first printer was declared broken, and went through many different repair tactics. The printer was cleaned, recalibrated, and had its resin completely recycled, but none of these attempts proved successful in returning the printer to its original state. For the final presentation of the project, the casings were FDM printed using a Prusa MK3 to allow for the final version of the arm to the robot.

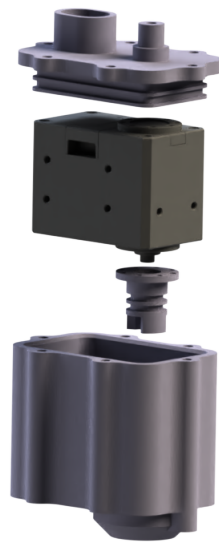


Figure 4.3: Case Lid, Dynamixel Servo, Servo Horn Extension, Case. Listed top to bottom.

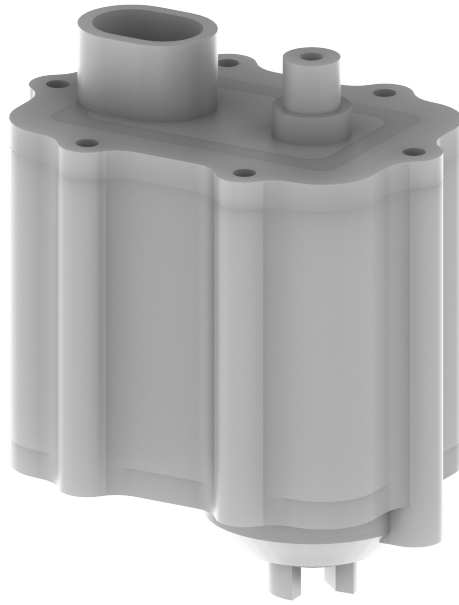


Figure 4.4: Assembled final case iteration, fabricated using SLA 3D printing technology.

4.2.1 Future Improvements

With a lack of time comes the inability to improve further. In the future, there are a few elements of the design that could be improved. The use of the BlueRobotics Penetrator bolt at the beginning was far less wasteful and allowed for more flexibility when assembling and disassembling the arm. Unfortunately, this task proved harder than expected given our current timeline.

In addition, finding a more reliable source of SLA printing would be necessary. SLA printing is vital to reliably make a water-tight casing. As of writing this report, we are waiting to hear back from the Advanced Prototyping Lab at Worcester Polytechnic Institute.

4.3 Fabricating Robot Arm

The nature of an underwater robotic arm necessitates a specialized design to mitigate the effects of its intended environment. The arm must be strong enough to function continuously without breaking, but light enough that the movement of the arm does not significantly change the center of gravity or inertia of the entire robotic system. Three main factors influence the design of the arm: viscosity of the environment, chemical properties of salt water, and how the fabrication method affects the structure of the arm.

The viscosity of water plays a role during the motion of the arm. Since water has a higher viscosity than air, measures must be taken to reduce the resistance of motion from the arm. For our application, this meant reducing the drag that the water imposed. To achieve this, we skeletonized each of the links to maintain the strength, while reducing surface area and allowing water to flow through the links. This reduced the effects of the arm's movements on

the rest of the robot. Skeletonization of the links also helps with the geometric strength of the part. Using this technique, the footprint of the part can be larger while using the same material, meaning that the profile of the part can take up a larger area. This same principle, in addition to other geometric structures, helps reduce the flex of the arm, decreasing the potential backlash imposed with long linkages.

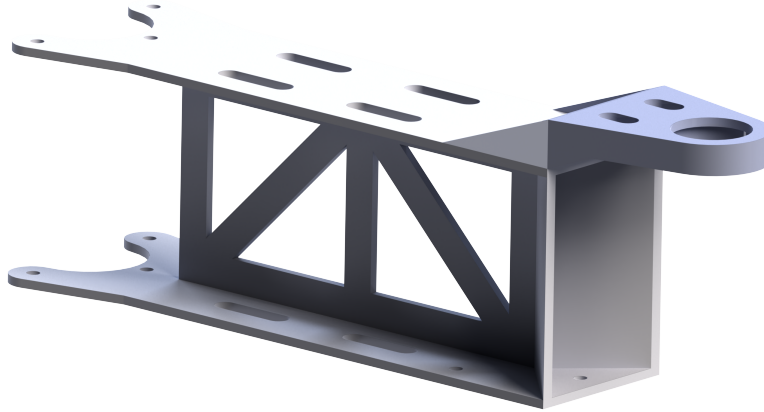


Figure 4.5: Link has been skeletonized to reduce weight, increase geometric strength, and reduce drag.

To improve rigidity and strength, and to reduce weight, we incorporated the servo casings into the structure of the arm, reducing material, providing structure to the links, and reducing the chance of torsion of the links. Furthermore, the hardware required to mount the linkage to the servo casing can also contribute to compressing, sealing, and increasing the stiffness of the servo casings. Incorporating the casings into the links allowed for the servos to be nested within the structure, further reducing the arm's footprint.

The arm was to be tested and used in both saltwater and chlorinated water. Both of these environments are solvents that have the potential to degrade plastics. Additionally, we needed a material that was stiff, resilient to impacts, and allowed for rapid prototyping. We chose to use PETG filament for FDM printing for quick, yet durable and chemically resistant parts. This resulted in parts that could be rapidly developed, tested, and with little cost associated with manufacturing.

Our use case required slight modifications to normal FDM printing techniques as we needed to adjust certain parameters that are not typical for conventional applications. In air, it is advantageous to have air pockets within the print. This allows for a lightweight print that has the same geometry as if created using other fabrication techniques, such as mold injection. Nevertheless, the presence of an air pocket in an underwater part poses challenges related to pressure and density. Assuming the part doesn't have any leaks and the structure

is indestructible, as the part increases in depth, the buoyancy would increase dramatically, creating issues in the movement of the BlueROV2. If the part is no longer assumed to be impermeable, this creates a situation where the part slowly leaks, letting water into the hollow pocket, and changing the buoyancy of the part as it fills or empties with water. This again, changes the movement patterns of the BlueROV2, creating further issues. Removing the assumption that these parts are indestructible, a large pressure difference between the inside of the part, and the outside of the part, may fail and lead to the destruction of said part. For these reasons, the part must be made solid and in-compressible, to avoid potential failure and destruction of the arm itself. Thus, in conjunction with the skeletonized nature of the arm, the links and casings were created with 100% infill to make them impervious to the pressure surrounding the parts, while keeping weight down and strength up.

Numerous small improvements were made to enhance the usability of the arm, alongside the integration of servo casings. Slots were added to the frame of the arm to allow for numerous cable tie attachment points along the links. This helps protect the cables from abrasion and snagging. Furthermore, bearing adapters are added as part of the attachment method to the servo casings. These are press-fit slots that allow for the link to attach with high stability to the casings with the use of a 608 bearing. The case is clamped between this attachment, and a second attachment plate that screws into the arm, as well as meshes with the servo horn extension.



Figure 4.6: Link with slots for cable ties, press fit bearing (Bottom Middle), and servo horn extension fitment (Bottom Right).

These aspects resulted in a compact, yet extendable, arm that is versatile underwater with a robust design.

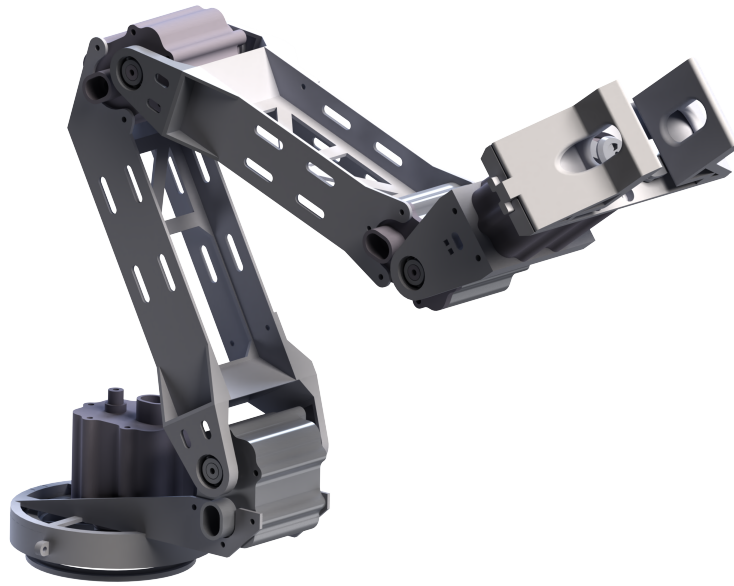


Figure 4.7: Final Arm Iteration, fabricated using FDM 3D printing technology.

4.3.1 Future Improvements

For future improvements, teams may make the arm stronger, reduce drag further, and allow for a larger reach, while achieving a more compact design. Currently, there is no scope encompassing these objectives due to time limitations. However, the goal of the arm was to make it as streamlined as possible while ensuring reliability across various use cases.

Chapter 5

Integration

5.1 Attaching the Arm to the ROV

The attachment of the arm onto the BlueROV2 is a quick and simple process. We used four M5x20 screws to attach the base of the arm to the frame of the robot, with a stability bearing (shown in Figure 5.1) that is located in the base of the arm. This bearing acts to remove any additional backlash that is associated with the base servo and to clamp the arm to the robot. Although this bearing gave the base a bigger footprint, it greatly reduces the

backlash of the entire arm, when paired to the camera of the BlueROV2.



Figure 5.1: Base of the arm that connects to ROV. Four M5 screw holes, stability bearing on the outside, and servo horn attachment in the center.

Regarding electronics, the arm's servos are connected in series. The wires were custom-built to fit the specific lengths of the arms using Blue Robotics marine grade wire and hand-crimped to fit JST EHR-3 connectors. This created a simple, yet effective, way to control each servo with a streamlined interface. This means that the entire arm can be controlled through a single wire that attaches the base servo to a single USB port located on the Raspberry Pi that is already used to control the movement of the BlueROV2. There is an inline adapter, known as the Dynamixel U2D2, that injects power from the battery and converts the signal from the USB connection to a serial connection that the Dynamixel servos require. This adapter utilizes the same voltage as the battery supplies, allowing for a simple and reliable connection. The wire that connects the base servo to the U2D2 module. Figure 5.2 shows a rendering of the fully-integrated robotic system.

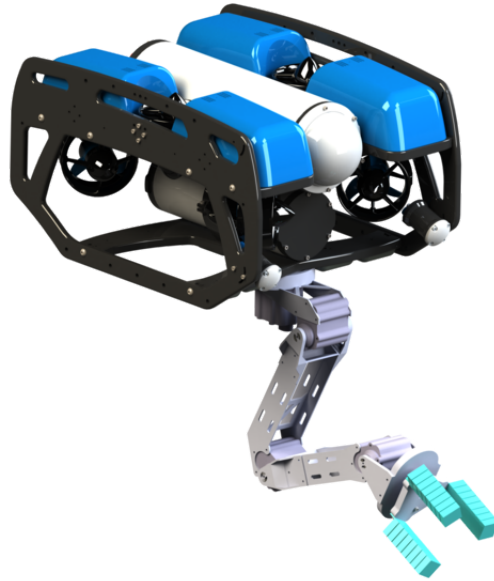


Figure 5.2: Robotic Arm attached to BlueROV2 with soft gripper.

5.2 Programming The Arm

To communicate with the arm, the ROV's onboard Raspberry Pi can take Python scripts, allowing for easy programming. Using Dynamixel's SDK, we send commands to the robot through an onboard USB port. To control the arm, we had to learn how to use the SDK, develop a position control scheme, incorporate the use of a gamepad to control the robotic arm intuitively and protect the arm from mis-inputs and over-extension.

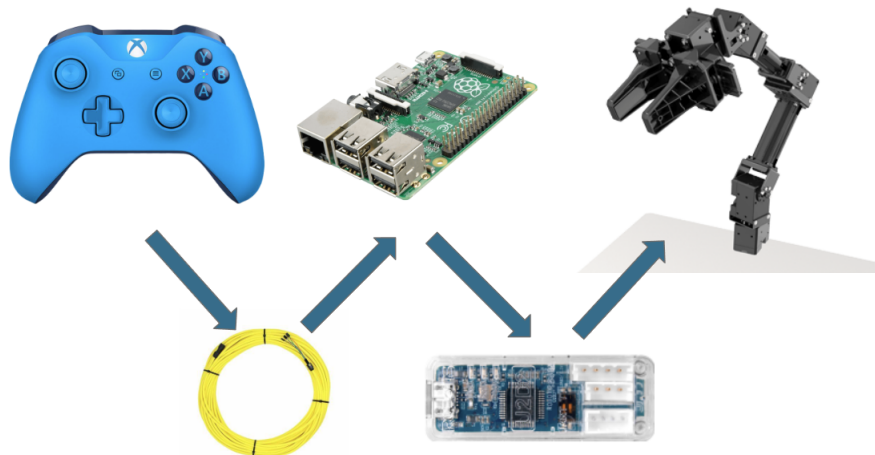


Figure 5.3: Electronic footprint of the system. Gamepad controller, Tether, Raspberry Pi, U2D2, Robotic Arm. Left to Right.

The Dynamixel SDK is a library comprised of communication protocols related to the reading and writing of individual servos on the arm. Each servo is individually addressable, meaning that we can control the exact position of each servo through the same interface on the Raspberry Pi. Using this communication method, we can update the positioning of the servos. To control the positioning of the end-effector, we utilized a polar coordinate system. We opted for this system as controlling the arm is much more intuitive for use with a controller.

We created a system of inverse kinematics equations to find the end-effector's polar coordinates using the theta, phi, and radius as the inputs. Since this is a four-degree-of-freedom arm, we calculated four equations to control the positioning of each servo. Due to the shape of the arm, the equations that were used corresponded to the "Elbow-Up" configuration of the arm. This means the arm only bends in one direction, allowing for specialized linkages and fewer calculations. These equations take in the goal position of the arm and calculate the angle needed for each servo to be rotated. Once this value is calculated, the program writes the desired position to the arm, and the servos move accordingly.

This technique of positioning the servos rather than controlling velocity helps reduce processing power. However, positional control also increases the lurching of the arm. For our tests and function, positional control works well to reduce battery consumption and create an arm that is very responsive to input.

We use the gamepad joysticks for inputting the new position of the arm. The "inputs" library in Python lends itself well to controller integration. In the case of polar coordinates, a single joystick can be used to control theta and phi (angles of the arm) while a pair of buttons can be used to control the radius that the arm extends. This piece of the program relies on a polling system that checks to see if any inputs are being submitted and whether or not these inputs need to be acted upon.

The Dynamixel servos do not have any built-in limit protection. Instead, they rely upon the amperage to determine only if their max torque limit has been reached. Unfortunately for the arm, and fortunately for the health of the servos, this maximum torque limit exceeds the strength of the PETG plastic. To protect the arm from over-extension and over-exertion, limits must be applied to limit the operating range of each servo. These horn angle values are found by moving the links to their limits and reading the values of the servos' current angles. These are then input as a threshold such that the program cannot write the angles above or below. This technique helps reduce the potential for problems when involved with over-straining the servos or destroying the links.

A flow chart representing the code structure for controlling the robotic arm is shown in Figure 5.4.

5.2.1 Future Programming Iterations

Improvements can be made to smoothen the movement of the arm, at the cost of processing power. Although positional control has advantages related to our use case, specifically in battery usage and responsiveness, it results in an arm that moves very jarringly. One way to fix this is to incorporate Jacobian velocity control. This technique would significantly smooth out the arm's movement at the cost of processing power. Another potential issue is that of communication loss. If communication is lost while the servo is set at a specific

velocity, there might not be the ability to stop the servos that are in motion. This issue requires development time that the team does not have. However, in the future, this may pose a viable solution, given precautionary and redundant programming.

Another potential solution is to have the position of the joysticks affect the velocity of the end-effector directly. In this case, rather than a position that the servos will be written to, the servos would instead be written an angular velocity to move at. This solution solves the jarring nature of the positional movement, however, it carries the same potential problem of communication loss associated with the Jacobian velocity control. Although this may be a potential solution, there very well might be others that are far more applicable to our scenario.

Chapter 6

Conclusion

These are the first steps in making a robotic system that can clean coral, utilizing a gripper that won't cause damage to the reefs. Combining the various aspects of the BlueROV2, robotic arm, and hydraulically actuated soft gripper allows for an effective system, can adapt, and even evolve for various applications not only limited to the ocean but any body of water.

Currently, the system is attached via a tether to a remotely operated gamepad controller. Using this interface, the robot can be switched between modes to manipulate the movement of the ROV or the arm and gripper. The progressively molded gripper is actuated hydraulically via a parasitic pump, while the arm will use the power supply of the onboard 12V battery to operate the independent servos.

The goal of the system is to be operated simply and effectively. Using the combination of the various components, coral reefs can be cleaned with less harm to the environment, and at a far more cost-effective rate.

Additionally, we present a novel fabrication technique for soft fluidic actuators. This process yielded a proof of concept and partial fabrication of actuators. With further investigation, this technique could cause great strides in soft robotics, as it would allow for softer versions of actuators with the quality of FDM 3D printed parts.

Bibliography

- [1] Y. Wang, M. Cai, S. Wang, X. Bai, R. Wang, and M. Tan, “Development and Control of an Underwater Vehicle–Manipulator System Propelled by Flexible Flippers for Grasping Marine Organisms,” *IEEE Transactions on Industrial Electronics*, vol. 69, pp. 3898–3908, Apr. 2022.
- [2] Z. E. Teoh, B. T. Phillips, K. P. Becker, G. Whittredge, J. C. Weaver, C. Hoberman, D. F. Gruber, and R. J. Wood, “Rotary-actuated folding polyhedrons for midwater investigation of delicate marine organisms,” *Science Robotics*, vol. 3, p. eaat5276, July 2018. Publisher: American Association for the Advancement of Science.
- [3] Z. Shen, H. Zhong, E. Xu, R. Zhang, K. C. Yip, L. L. Chan, L. L. Chan, J. Pan, W. Wang, and Z. Wang, “An Underwater Robotic Manipulator with Soft Bladders and Compact Depth-Independent Actuation,” *Soft Robotics*, vol. 7, pp. 535–549, Oct. 2020. Publisher: Mary Ann Liebert, Inc., publishers.
- [4] X. Shi, C. Zhu, and P. Lu, “Design and control of underwater robot system for sea cucumber fishing,” *International Journal of Advanced Robotic Systems*, vol. 19, p. 17298806221077625, Jan. 2022. Publisher: SAGE Publications.
- [5] Z. Gong, B. Chen, J. Liu, X. Fang, Z. Liu, T. Wang, and L. Wen, “An Opposite-Bending-and-Extension Soft Robotic Manipulator for Delicate Grasping in Shallow Water,” *Frontiers in Robotics and AI*, vol. 6, 2019.
- [6] G. Picardi, M. De Luca, G. Chimienti, M. Cianchetti, and M. Calisti, “User-Driven Design and Development of an Underwater Soft Gripper for Biological Sampling and Litter Collection,” *Journal of Marine Science and Engineering*, vol. 11, p. 771, Apr. 2023. Number: 4 Publisher: Multidisciplinary Digital Publishing Institute.
- [7] D. Herrero-Pérez and H. Martínez-Barberá, “Soft Gripper Design and Fabrication for Underwater Grasping,” *Applied Sciences*, vol. 12, p. 10694, Jan. 2022. Number: 21 Publisher: Multidisciplinary Digital Publishing Institute.
- [8] N. R. Sinatra, C. B. Teeple, D. M. Vogt, K. K. Parker, D. F. Gruber, and R. J. Wood, “Ultragentle manipulation of delicate structures using a soft robotic gripper,” *Science Robotics*, vol. 4, p. eaax5425, Aug. 2019. Publisher: American Association for the Advancement of Science.

- [9] K. Galloway, C., K. P. Becker, B. T. Phillips, J. Kirby, S. Licht, D. Tchernov, R. J. Wood, and D. F. Gruber, “Soft Robotic Grippers for Biological Sampling on Deep Reefs,” *Soft Robotics*, vol. 3, pp. 1–42, Mar. 2016.
- [10] A. Billard and D. Kragic, “Trends and challenges in robot manipulation,” *Science*, vol. 364, p. eaat8414, June 2019.
- [11] D. M. Vogt, K. P. Becker, B. T. Phillips, M. A. Graule, R. D. Rotjan, T. M. Shank, E. E. Cordes, R. J. Wood, and D. F. Gruber, “Shipboard design and fabrication of custom 3D-printed soft robotic manipulators for the investigation of delicate deep-sea organisms,” *PLOS ONE*, vol. 13, p. e0200386, Aug. 2018. Publisher: Public Library of Science.
- [12] Y. Zhang, D. Kong, Y. Shi, M. Cai, Q. Yu, S. Li, K. Wang, and C. Liu, “Recent progress on underwater soft robots: adhesion, grabbing, actuating, and sensing,” *Frontiers in Bioengineering and Biotechnology*, vol. 11, p. 1196922, Aug. 2023.
- [13] T. J. Wallin, J. Pikul, and R. F. Shepherd, “3D printing of soft robotic systems,” *Nature Reviews Materials*, vol. 3, pp. 84–100, June 2018. Publisher: Nature Publishing Group.
- [14] S. V. Kendre, G. T. Teran, L. Whiteside, T. Looney, R. Wheelock, S. Ghai, and M. P. Nemitz, “Printable flexible robots for remote learning,” American Society of Engineering Education, April 2022.
- [15] F. Schmitt, O. Piccin, L. Barbé, and B. Bayle, “Soft Robots Manufacturing: A Review,” *Frontiers in Robotics and AI*, vol. 5, 2018.
- [16] H. T. Pinheiro, C. MacDonald, R. G. Santos, R. Ali, A. Bobat, B. J. Cresswell, R. Francini-Filho, R. Freitas, G. F. Galbraith, P. Musembi, T. A. Phelps, J. P. Quimbayo, T. E. A. L. Quiros, B. Shepherd, P. V. Stefanoudis, S. Talma, J. B. Teixeira, L. C. Woodall, and L. A. Rocha, “Plastic pollution on the world’s coral reefs,” 2023.
- [17] NOAA, “Coral reef ecosystems.”
- [18] R. Akhtar, M. Y. Sirwal, K. Hussain, M. A. Dar, M. Shahnawaz, and Z. Daochen, “Impact of plastic waste on coral reefs: An overview,” 2022.
- [19] D. Friends, “Quarterly clean-up dive.”
- [20] S. Zhang, X. Ke, Q. Jiang, Z. Chai, Z. Wu, and H. Ding, “Fabrication and Functionality Integration Technologies for Small-Scale Soft Robots,” *Advanced Materials*, vol. 34, no. 52, p. 2200671, 2022. eprint: <https://onlinelibrary.wiley.com/doi/pdf/10.1002/adma.202200671>.
- [21] F. C. P. Sales, R. M. Ariati, V. T. Noronha, and J. E. Ribeiro, “Mechanical Characterization of PDMS with Different Mixing Ratios,” *Procedia Structural Integrity*, vol. 37, pp. 383–388, Jan. 2022.

- [22] H.-T. Lin, G. G. Leisk, and B. Trimmer, “GoQBot: a caterpillar-inspired soft-bodied rolling robot,” *Bioinspiration & Biomimetics*, vol. 6, p. 026007, June 2011.
- [23] C. Lee, M. Kim, Y. J. Kim, N. Hong, S. Ryu, H. J. Kim, and S. Kim, “Soft robot review,” *International Journal of Control, Automation and Systems*, vol. 15, pp. 3–15, Feb. 2017.
- [24] R. Industries, “Filaflex.” Recreus.
- [25] NinjaTek, “Shop.”
- [26] Elastollan, “Think, create, elastollan® (tpu).”
- [27] E. Sachyani Keneth, A. Kamyshny, M. Totaro, L. Beccai, and S. Magdassi, “3D Printing Materials for Soft Robotics,” *Advanced Materials*, vol. 33, no. 19, p. 2003387, 2021. [.eprint: https://onlinelibrary.wiley.com/doi/pdf/10.1002/adma.202003387](https://onlinelibrary.wiley.com/doi/pdf/10.1002/adma.202003387).
- [28] X. Dong, X. Luo, H. Zhao, C. Qiao, J. Li, J. Yi, L. Yang, F. J. Oropeza, T. Shihao Hu, Q. Xu, and H. Zeng, “Recent advances in biomimetic soft robotics: fabrication approaches, driven strategies and applications,” *Soft Matter*, vol. 18, no. 40, pp. 7699–7734, 2022. Publisher: Royal Society of Chemistry.
- [29] F. Xu, H. Wang, K. W. S. Au, W. Chen, and Y. Miao, “Underwater Dynamic Modeling for a Cable-Driven Soft Robot Arm,” *IEEE/ASME Transactions on Mechatronics*, vol. 23, pp. 2726–2738, Dec. 2018. Conference Name: IEEE/ASME Transactions on Mechatronics.
- [30] H. Yan, Y. Wang, W. Shen, F. Li, G. Gao, T. Zheng, Z. Xu, S. Qian, C.-y. Chen, C. Zhang, G. Yang, and T. Chen, “Cable-Driven Continuum Robot Perception Using Skin-Like Hydrogel Sensors,” *Advanced Functional Materials*, vol. 32, no. 34, p. 2203241, 2022. [.eprint: https://onlinelibrary.wiley.com/doi/pdf/10.1002/adfm.202203241](https://onlinelibrary.wiley.com/doi/pdf/10.1002/adfm.202203241).
- [31] J. I. Lipton, R. MacCurdy, Z. Manchester, L. Chin, D. Cellucci, and D. Rus, “Handedness in shearing auxetics creates rigid and compliant structures,” *Science*, vol. 360, pp. 632–635, May 2018. Publisher: American Association for the Advancement of Science.
- [32] R. J. Wood, S. Avadhanula, R. Sahai, E. Steltz, and R. S. Fearing, “Microrobot Design Using Fiber Reinforced Composites,” *Journal of Mechanical Design*, vol. 130, Mar. 2008.
- [33] Q. Ze, S. Wu, J. Nishikawa, J. Dai, Y. Sun, S. Leanza, C. Zemelka, L. S. Novelino, G. H. Paulino, and R. R. Zhao, “Soft robotic origami crawler,” *Science Advances*, vol. 8, p. eabm7834, Mar. 2022. Publisher: American Association for the Advancement of Science.
- [34] S. Liu, Y. Zhu, Z. Zhang, Z. Fang, J. Tan, J. Peng, C. Song, H. H. Asada, and Z. Wang, “Otaridae-Inspired Soft-Robotic Supernumerary Flippers by Fabric Kirigami and Origami,” *IEEE/ASME Transactions on Mechatronics*, vol. 26, pp. 2747–2757, Oct. 2021. Conference Name: IEEE/ASME Transactions on Mechatronics.

- [35] A. Rafsanjani, Y. Zhang, B. Liu, S. M. Rubinstein, and K. Bertoldi, “Kirigami skins make a simple soft actuator crawl,” *Science Robotics*, vol. 3, p. eaar7555, Feb. 2018. Publisher: American Association for the Advancement of Science.
- [36] A. Pal, D. Goswami, and R. V. Martinez, “Elastic Energy Storage Enables Rapid and Programmable Actuation in Soft Machines,” *Advanced Functional Materials*, vol. 30, no. 1, p. 1906603, 2020. eprint: <https://onlinelibrary.wiley.com/doi/pdf/10.1002/adfm.201906603>.
- [37] G. Stano, L. Arleo, and G. Percoco, “Additive Manufacturing for Soft Robotics: Design and Fabrication of Airtight, Monolithic Bending PneuNets with Embedded Air Connectors,” *Micromachines*, vol. 11, p. 485, May 2020. Number: 5 Publisher: Multidisciplinary Digital Publishing Institute.
- [38] Z. J. Patterson, A. P. Sabelhaus, K. Chin, T. Hellebrekers, and C. Majidi, “An untethered brittle star-inspired soft robot for closed-loop underwater locomotion,” Aug. 2020. arXiv:2003.13529 [cs].
- [39] J. R. Tumbleston, D. Shirvanyants, N. Ermoshkin, R. Januszewicz, A. R. Johnson, D. Kelly, K. Chen, R. Pinschmidt, J. P. Rolland, A. Ermoshkin, E. T. Samulski, and J. M. DeSimone, “Continuous liquid interface production of 3D objects,” *Science*, vol. 347, pp. 1349–1352, Mar. 2015. Publisher: American Association for the Advancement of Science.
- [40] Formlabs, “Materials catalog.”
- [41] S. Schlatter, G. Grasso, S. Rosset, and H. Shea, “Inkjet Printing of Complex Soft Machines with Densely Integrated Electrostatic Actuators,” *Advanced Intelligent Systems*, vol. 2, no. 11, p. 2000136, 2020. eprint: <https://onlinelibrary.wiley.com/doi/pdf/10.1002/aisy.202000136>.
- [42] M. A. Shah, D.-G. Lee, B.-Y. Lee, and S. Hur, “Classifications and Applications of Inkjet Printing Technology: A Review,” *IEEE Access*, vol. 9, pp. 140079–140102, 2021.
- [43] K. Liu, W. Chen, W. Yang, Z. Jiao, and Y. Yu, “Review of the Research Progress in Soft Robots,” *Applied Sciences*, vol. 13, p. 120, Jan. 2023. Number: 1 Publisher: Multidisciplinary Digital Publishing Institute.
- [44] ANNIMOS, “Digital servo 25kg.”
- [45] B. T. Engineering, “Underwater servo ser-20xx.”
- [46] C. Duran, V. Subbian, M. T. Giovanetti, J. R. Simkins, and F. R. B. Jr, “Experimental desktop 3d printing using dual extrusion and water-soluble polyvinyl alcohol,” *Rapid Prototyping Journal*, vol. 21, p. 528–534, Jan. 2015.
- [47] T. L. Brooks-Richards, N. C. Paxton, M. C. Allenby, and M. A. Woodruff, “Dissolvable 3d printed pva moulds for melt electrowriting tubular scaffolds with patient-specific geometry,” *Materials Design*, vol. 215, p. 110466, Mar. 2022.

- [48] “The printer does not resume printing after a pause.” Post on Original Prusa 3D Printers forum by user max.
- [49] Dynamixel, “Dynamixel xm430-w350-r.”